

Radiocesium concentrations in soil and leaf after decontamination practices in a forest plantation highly polluted by the Fukushima accident

Manuel López-Vicente ^{1,2,*}, Yuichi Onda ², Junko Takahashi ², Hiroaki Kato ², Shinya Chayama ³, Keigo Hisadome ³

¹ Department of Soil and Water, Experimental Station of Aula Dei, EEAD-CSIC. Avda. Montañana 1005, 50059 Zaragoza, Spain.

² Center for Research in Isotopes and Environmental Dynamics, University of Tsukuba. Tsukuba, Ibaraki 305-8572, Japan.

³ Geo-Environmental Department, Asia Air Survey Co., LTD. Kawasaki-City, Kanagawa, Japan.

*Corresponding author (M. López-Vicente). E-mail: mvicente@eead.csic.es; Tel.: +34 976 716124; Website: <http://digital.csic.es/cris/rp/rp03203>

Received 3 November 2017, Revised 15 February 2018, **Accepted 9 April 2018**, Available online

19 April 2018: <https://www.sciencedirect.com/science/article/pii/S0269749117345906>

Published online in Elsevier ScienceDirect: <https://doi.org/10.1016/j.envpol.2018.04.045>

***Environmental Pollution* 239 (August 2018), 448–456**

ABSTRACT

Owing to the Fukushima Dai-ichi Nuclear Power Plant (FDNPP) accident a vast amount of radiocesium was released polluting the land. Afterwards, a variety of decontamination practices has been done, reducing the ambient dose rates. In this study we evaluated the effectiveness of eight forest decontamination practices by means of monitoring the radiocesium (¹³⁷Cs) concentration in soil and leaf samples, and the daily discharge rates in ten plots during 27 months (May 2013 - July 2015). A forest plantation located 16 km southwest to the FDNPP and within the exclusion area was selected. Radiocesium concentrations were analysed using a germanium gamma ray detector. The differences in radiocesium activities between the different plots were statistically significant ($p < 0.05$) and four homogeneous groups were distinguished. Tree thinning and litter removal greatly reduced the radioactivity and the two plots devoted to

these practices presented the highest discharge rates of ^{137}Cs (Th+LR; 350–380 Bq / m² day), followed by the two Th plots (163–174 Bq / m² day). The clearcutting with LR and the LR plots (104 and 92 Bq / m² day) also had higher rates than those rates in the control plots (51 Bq / m² day). We only observed low rates in the two plots with matting (19–25 Bq / m² day). The temporal variability was explained by (i) the different rainfall depths registered during the measurement intervals (accumulated precipitation from 14 to 361 mm); and (ii) the fluctuations of the total surface coverage. The decrease trend in radiocesium concentration was high in 2013, moderate in 2014 and low in 2015 owing to the vegetation recovery after the countermeasures, thus reducing the possibility of the second pollution of the neighbouring areas. The average proportions of contribution of ^{137}Cs discharge by soil and leaf fraction were 96.6% and 3.4%.

Capsule: The highest discharge rates of Cs-137 appeared in the two plots devoted to tree thinning and litter removal. We only observed low rates in the two plots with matting.

Keywords: Fukushima accident; Radiocesium; Clearcutting; Litter removal; Tree thinning.

1. Introduction

On 11 March 2011 a 9.0 earthquake and the resulting tsunami occurred in central-eastern Japan triggering, one day after, the Fukushima Dai-ichi Nuclear Power Plant (FDNPP) accident. After failure of the cooling systems, several hydrogen explosions damaged three of the six nuclear reactors of the power plant on March 12, 14 and 15, and affected a fourth reactor which had already been stopped (Achim et al., 2014). Published estimates suggest total release amounts of 12–36.7 PBq of ^{137}Cs (with $^{134}\text{Cs}/^{137}\text{Cs}$ approximately equal to 1.0) and 150–160 PBq of ^{131}I (Aliyu et al., 2015). Despite the bulk of radionuclides were transported offshore and out over the Pacific Ocean, significant wet and dry deposits of those radionuclides occurred on land (ca. 22%) (Morino et al., 2011). The most affected areas are in Fukushima Prefecture (Fuk-Pref, hereafter) and in a minor way in Miyagi, Tochigi, Gunma and Ibaraki Prefectures. Initial fallout contaminated cultivated soils, forests, water bodies, residential areas, asphalt and concrete surfaces, and significant pollution still remains (Saito et al., 2014; Mikami et al., 2015). After the accident, a variety of decontamination practices (soil removal in paddies, forests and schoolyards, litter removal, etc.) has been done, reducing the ambient dose rates (Hashimoto et al., 2012; Saegusa et al., 2015; Yang et al., 2016). This accident caused important economic

damages that include, among others, the cost of decontamination practices, and the abandonment of cultivated and residential areas (Yasutaka and Naito, 2016). Additionally, there is a significant concern about the environmental and health consequences at short, medium and long-term (Aliyu et al., 2015).

Due to the strong adsorption capability of radiocesium to soil particles and vertical soil migration, seven weeks after the accident 86% of total radiocesium absorbed in the soil profile were accumulated in the upper 2.0 cm in the cultivated soils located near the FDNPP (Kato et al., 2012a). After 5 months of the initial fallout, more than 60% of the total deposited radiocesium (^{134}Cs and ^{137}Cs) in coniferous forest plantations of cypress and cedar remained in the canopy. The half lives of ^{137}Cs absorbed in the cypress and cedar canopies were calculated as 620 days and 890 days, respectively for the period of 0–160 days. The transfer of the deposited radiocesium from the canopy to the forest floor was slow compared with that of the spruce forest affected by fallout from the Chernobyl nuclear reactor accident (Kato et al., 2012b). Between 17 days and 7 months after the accident, the transfer of radiocesium from the canopy of a coniferous forest to the forest floor via throughfall and stemflow was predominant in the first weeks. However, the contributions of hydrological pathways became less important as time passed, and the litterfall route became more important (Teramage et al., 2014a). From July to September 2011 (<200 d after the initial fallout) the deposition of ^{137}Cs to the forest floor occurred mainly in throughfall during the first rainy season, thereafter (from Sep'2011 to Dec'2012), the transfer of ^{137}Cs from the canopy to forest floor occurred mainly through litterfall (Kato et al., 2017). Teramage et al. (2014a) observed that 99% of the total soil inventory of the pre- and Fukushima derived ^{137}Cs was in the upper 10 cm in a representative coniferous forest soil. On the other hand, most radiocesium in the tree rings was directly absorbed from the atmosphere via bark and leaves rather than via roots; and xylem ^{137}Cs concentrations will not be affected by root uptake if active root systems occur 10 cm below the soil (Mahara et al., 2014).

On December 2012, 22 months after the accident, Matsuda et al. (2015) found that radioactive cesium remained within 5 cm of the ground surface at most study sites (71 sites) within a 100-km radius of the FDNPP. These authors calculated a downward migration rate ranging between 1.7 and 9.6 kg m⁻² y⁻¹. Two years after the FDNPP accident the downward migration of radiocesium to subsurface soil (5-10 cm) was only significant (26% of the total ^{137}Cs) in paddy fields near Kawamata Town (Takahashi et al., 2015). In other land uses in the Fuk-Pref, such as abandoned farmlands and tobacco fields, pastures, meadows, mixed forest, and mature and young cedar, ^{137}Cs was strongly adsorbed by soil particles and rarely migrated downward as soluble form.

In Fuk-Pref, sediment fingerprinting approaches have confirmed an effective radiocesium migration from upstream areas to coastal plains due to rainfall and spring flood events (Lepage et al., 2016). Iwagami et al. (2017a) calculated that the total annual ^{137}Cs discharge by suspended sediment, coarse organic matter, and dissolved fractions from a headwater catchment located ~35 km northwest of FDNPP was 0.02–0.3% of the total initial deposition. The total flux of radiocesium into the Pacific Ocean from the river systems and estimated at outlet stations was significant, especially during the typhoon period during the first year after the accident (Yamashiki et al., 2014). Kinouchi et al. (2015) simulated with WEP (Water and Energy transfer Process model) and calculated the long-term change in ^{137}Cs remaining in the headwater areas near the FDNPP due to the erosion and transport of contaminated sediments. These processes will reduce the amount of ^{137}Cs remaining in the catchment to 39% of the initial amount of deposition within 30 y from 2014 on, which results in the effective half-life of ^{137}Cs to be approximately 22 years.

Since the occurrence of the FDNPP accident until now the overall concentrations of ^{134}Cs ($t_{1/2} = 2.07$ years) and ^{137}Cs ($t_{1/2} = 30.17$ years) in soils, natural vegetation and crops, runoff (suspended and dissolved particles), stream water and groundwater have decreased due to the natural decay of the radionuclides as well as due to the implementation of decontamination practices. Easily applicable decontamination methods for various school facilities in Fuk-Pref included removing topsoil from schoolyards and purification of pool water (Saegusa et al., 2015). From June 2011 to July 2013 a declining trend of dissolved ^{137}Cs concentrations in stream water and groundwater (at a depth of 30 m) was observed in headwater catchments located ~35 km north west of FDNPP (Iwagami et al., 2017b). These authors also reported that the concentration of dissolved ^{137}Cs in stream water increased temporarily during the rainfall events. In cultivated soils near Kawamata Town (Fuk-Pref), the radiocesium accumulation in rice plant decreased with time (2012-2014) in both control and decontaminated fields (Yang et al., 2016). Although decontamination practices effectively reduced ^{134}Cs and ^{137}Cs concentrations (ca. 80% lower) in tadpoles in rice paddies, radiocesium concentrations in the decontaminated surface paddy soils became 3.8 times greater one year after decontamination due to the subsequent movement of radiocesium from adjacent areas (Sakai et al., 2014).

More than 70% of the Japanese archipelago is covered by forest, of which 60% is evergreen coniferous forest (Onda et al., 2010). This is also true in the highly contaminated area (≥ 1000 kBq m^{-2}), where 66% of the area is covered by forest (Hashimoto et al., 2012). However, specific studies on decontamination practices in forest areas affected by the FDNPP accident are less common in the literature. Hashimoto et al. (2012) suggested that removing litter is an efficient

method of decontamination in forest areas in Fuk-Pref, although litter is being continuously decomposed, and contaminated leaves will continue to fall on the soil surface for several years; hence, the litter should be removed promptly but continuously before more radioactive elements are transferred into the soil. Iijima et al. (2013) tested different decontamination techniques proposed by the Japan Atomic Energy Agency (JAEA) in a forest dominated by Japanese cedar trees and fir trees located 1.3 km southwest of the FDNPP. These authors found that cutting down and removing trees in the outermost area (10-m width) of the forest as well as stripping contaminated topsoil of the forest floor and pruning the trees slightly decreased the radiocesium (^{134}Cs and ^{137}Cs) dose rates. Yasutaka et al. (2013) calculated that remove fallen leaves and litter layer of 20% area of each 100 m-mesh in forest (adjacent buildings, paddy fields and other agricultural land mesh units) areas in the Evacuation Zone and Planned Evacuation Zone (restricted zone, about 1100 km²) in Fuk-Pref had an average decontamination efficiency between 19 and 59% in air dose rates ranging between less than 1 to more than 10 $\mu\text{Sv h}^{-1}$, respectively. Recently, Cresswell et al. (2016) reported that clearing trees and applying wood chips from timber reduced dose rates by 10–15% beyond that achieved by just clearing the forest litter and natural redistribution of radiocaesium in a contaminated forest near Kawamata town (Fuk-Pref).

The basic scenario of decontamination in Fuk-Pref included forested areas within 20 m of habitation areas. Implementing decontamination of all forested areas will provide some major reductions in the external radiation dose for the average inhabitant, although decontamination costs could potentially exceed JPY16 trillion (Yasutaka and Naito, 2016). This extraordinary cost and the scarcity of specific previous publications make necessary further studies about the effectiveness of forest decontamination policies and practices. We hypothesize that litter removal, tree thinning and the combination of both practices, trigger different effects on modifying the natural discharge rates of radiocesium in a forested hillslope. In this study, we aim to clear the effect of eight decontamination practices (mainly litter removal with and without clearcutting, tree thinning with and without logged areas, and the combination of both) of ^{137}Cs in a Japanese cedar plantation located 16 km southwestern from the FDNPP and within the exclusion area. The soil and leaf weight and the radiocesium discharge rates were monitored during 27 months (from May 2013 to July 2015) in a set of ten experimental plots (5 x 2 m per plot; 100 m² in total) and radioactivities were determined in the soil and litter fractions. This study will contribute to understand the future behaviour of the radiocesium budget in the Japanese polluted areas, especially in the forested headwaters that supply fresh water in Fuk-Pref and within the exclusion area.

2. Material and methods

2.1. Study area

This study was done in the stand A (37° 20' 04" N, 140° 53' 14" E) of the Kawauchi experimental site, composed by a forest plantation of Japanese cedar (*Cryptomeria japonica*) and natural understory vegetation. This plantation has an age of 58 years (in 2017) and is located in a steep hillslope (average slope of 25°) near Kawauchi village, in the Fukushima Prefecture (northern Japan) at 16 km southwest to the FDNPP and within the exclusion area. The study area occupies 1 ha and includes ten runoff plots that are managed by the Fukushima Prefectural Forestry Research Centre. Each plot covers 10 m² (5 m x 2 m) and has a rectangular shape with the largest side parallel to the maximum slope. The soils were classified as Andosols (Takahashi et al., 2015). Climate is humid with an annual rainfall depth of 1736 mm year⁻¹. The region has two dominant storm periods, the Baiu season from late June to mid-July, and the typhoon season from late August through October. Rainy season precipitation (from July to October) accounts more than half of the mean annual precipitation. The total surface deposition of ¹³⁴⁺¹³⁷Cs in the study area reached 1,110 kBq m⁻² (based on the 3rd airborne monitoring survey by MEXT, Japan; <http://www.radioactivity.nsr.go.jp/en/>; Supplementary Fig. 1). The air radiation dose rate measured at 1-m above ground and before plots' installation (November 2012) ranged between 2.4~5.0 μSv h⁻¹ (internal report of Asia Air Survey Co., LTD.). In a previous and recent study the radiocesium was determined in > 92% of the mushrooms within the Kawauchi county, reaching high and very high values (between 100 and > 1,000 Bq kg⁻¹) of ¹³⁴⁺¹³⁷Cs in a model stand near our study area (Orita et al., 2017).

2.2. Decontamination practices, data collection and test-period

The main forest management operations (FMO) included litter removal (LR), tree thinning (Th), and clearcutting (CC). In total, eight different options and combinations of these practices were done. FMO were done before installing the plots, between December 2012 and July 2013 (Table 1). The plots were installed on April and July 2013 and measurements started on May 2013. One plot was devoted to litter removal; two plots to tree thinning without litter removal (Th_1 with logged area, and Th_2 under remnant trees); two plots to tree thinning with litter removal (Th+LR_1 with logged area, and Th+LR_2 under remnant trees); and three plots to clearcutting with litter removal (CC+LR_1 without matting, CC+LR_2 matting with seeds, and

CC+LR_3 matting without seeds). Finally, two plots (Co_1 and Co_2) remained as control plots without application of any decontamination practice (Supplementary Fig. 2). The average slope steepness of the plots was 21°, ranging between 8° and 37°. Each plot had a gauging station where overland flow (runoff, sediment and litter) was stored between each field survey. The test period covered 27 months, from May 2013 to July 2015, and soil and leaf samples were collected at each plot during 39 field surveys. The average period between each survey lasted on average 21 days (every 16 days during the first 12 months, and every 29 days in the next 15 months).

The percentages of the physical coverage on the ground (SC) and the ground coverage by vegetation (CC) presented changed over the test period (Fig. 1). Because of the FMO the minimum percentages of SC and CC appeared between May and July 2013, and low values were observed between January and April 2014, and between January and April 2015. Owing to the natural vegetation recovery the maximum combined percentages of SC and CC appeared in July 2015, and high values were observed between September and October 2013, and between July and September 2014.

2.3. Laboratory analysis

Sediment samples were collected from the plots by the staff of the company Asia Air Survey Co., Ltd. (Geo-Environmental Department, Kawasaki-City, Kanagawa, Japan). Then, the soil and litter fractions were separated from each sample. Gamma-ray emissions at energy of 661.6 keV (¹³⁷Cs) were measured using a germanium semiconductor detector at the University of Tsukuba (GC4019, Canberra), and then the radiocesium concentrations were determined in the soil and litter fractions. The physical decay of ¹³⁷Cs was corrected to the sampling date (more details in Iwagami et al., 2017c). Then, the inventory (Bq m⁻²) and daily inventory (Bq m⁻² day⁻¹) of ¹³⁷Cs activity in the soil and leaf samples were calculated.

2.4. Statistical analysis

Data were checked for normality using the Shapiro–Wilk test and since normality test failed, statistical differences in mean values between the eight decontamination practices and the control plots were calculated by means of the analysis of variance (ANOVA; one-way with repeated measures using the Holm-Sidak test) of: (i) the ¹³⁷Cs activities; (ii) the ¹³⁷Cs inventory and (iii) the daily discharge rates in the leaf and soil samples of the ten plots. The differences

among the treatment groups were estimated at 0.0001 and 0.001 levels. All statistical analyses were performed using SigmaPlot software (version 13.0) for Windows (Systat Software Inc., 2014). Additionally, box plots displaying the full range of variation of radiocesium activities and inventory, and of the daily discharge rates in the different plots were generated.

3. Results and discussion

3.1. Evolution of sediment discharge and radiocesium activity

The amount of soil and leaf collected in the ten plots clearly varied over the test period and between the different plots (Fig. 2.a). As the soil and leaf samples were collected during 39 time-integrated surveys that comprised 294 rainfall events and the duration of each runoff event was not monitored, the discharge rates were estimated on the basis of each survey. The highest discharge rates were observed in the Th+LR_1 (mean 9.2 and 343.7 g survey⁻¹ of leaf and soil), Co_1 (51.0 and 231.3 g survey⁻¹), LR (35.2 and 232.4 g survey⁻¹) and Th_2 (23.1 and 220.8 g survey⁻¹) plots. The lowest rates appeared in the CC+LR_3 (12.2 and 63.6 g survey⁻¹), Co_2 (24.8 and 29.3 g survey⁻¹) and CC+LR_2 (8.5 and 25.8 g survey⁻¹) plots. Intermediate rates were registered in the Th+LR_2 (7.3 and 176.4 g survey⁻¹), CC+LR_1 (13.8 and 130.6 g survey⁻¹) and Th_1 (9.1 and 138.3 g survey⁻¹) plots. The variability between the two control plots was explained by the effect of the different slope (75% higher in Co_1 related to the slope in Co_2). The high discharge rates observed in the LR plot can be also explained by its high slope (37°). Despite the low slope (17°) in the Th+LR_1, this plot had the highest discharge rates owing to its FMO (logged area without remnant trees). Conversely, the presence of matting explained the low rates observed in the CC+LR_2 and CC+LR_3 plots. The coefficients of variation (CV) ranged between 108% (Th_1) and 199% (CC+LR_2) for the leaf discharge rates and between 93% (Th_2) and 325% (CC+LR_3) for the soil discharge rates. These CV described a high temporal variability that can be explained by (i) the different rainfall depths registered during the measurement intervals (from 14 to 361 mm interval⁻¹; mean 128 mm interval⁻¹); and (ii) the marked fluctuations of the total surface coverage (TSC) between the periods with minimum (ca. 0%) and maximum (ca. 100%) coverage (Fig. 1). When TSC was lower than average (TSC_min), the dry weight of leaf was higher in nine out of ten plots (140% on average) than the dry weight obtained when the TSC was higher than average (TSC_max). This trend was mirrored in six out of ten plots (2% lower on average) related to the soil samples. However, no significant decreasing or increasing trend was observed in the overland flow (leaf and soil) yield (dry weight) over the study period (Fig. 3.a).

The ^{137}Cs activities ranged between 1,000 and 120,000 $\text{Bq kg}^{-1} \text{ survey}^{-1}$ in the leaf (mean 31,848 $\text{Bq kg}^{-1} \text{ survey}^{-1}$) samples and between 6,000 and 120,000 $\text{Bq kg}^{-1} \text{ survey}^{-1}$ in the soil (mean 31,924 $\text{Bq kg}^{-1} \text{ survey}^{-1}$) samples (Fig. 2.b). The differences in radiocesium activities between the different plots were statistically significant ($p < 0.05$) and four homogeneous groups were distinguished: the control and the Th_2 plots had the highest values of radiocesium activities in both the leaf and soil samples, the CC+LR_3 plot had the lowest values in all cases, and the CC+LR_1, CC+LR_2 and Th+LR_2 plots had intermediate values (Table 2). The LR, Th_1 and Th+LR_1 plots showed greater variability (see box plots in Supplementary Fig. 3). None significant correlation was observed among the dry weight of the leaf and soil samples and their corresponding values of ^{137}Cs activities, except in the Th+LR_1 plot where positive and significant ($p < 0.0001$) linear correlation was obtained among the dry weight of the soil samples and the ^{137}Cs (Pearson's r : 0.700) activities. These results suggested that radiocesium activities were not dependent on the amount of overland flow except in the plot with the highest overland flow yield. The values of ^{137}Cs activities in the leaf and soil samples were influenced by the total surface coverage (TSC) factor (Table 3). Despite the high coefficients of variability observed in the values of ^{137}Cs activities in the leaf and soil samples, the mean and median values were quite similar between them at each plot and sample type. During TSC_min the radiocesium activity was 29% higher in the leaf samples than during TSC_max. Conversely, the ^{137}Cs activity in the soil samples was 12% lower during TSC_min than during TSC_max. A decreasing trend in the radiocesium concentration was observed in the plots with decontamination practices, with average Pearson's coefficients of 0.570 in $^{137}\text{Cs}_{\text{leaf}}$, and 0.607 in $^{137}\text{Cs}_{\text{soil}}$. Moreover, the decrease in radiocesium concentration in 2013 and the first half of 2014 was higher than the decrease observed in the second half of 2014 and the first half of 2015 owing to the continuous vegetation recovery after the decontamination practices (Fig. 3.b).

3.2. Daily movement of radiocesium and effectiveness of the decontamination practices

The evolution in the ^{137}Cs inventories in the soil and leaf samples over the test period was analysed in the ten plots (Fig. 4). Values in the leaf samples ranged between 0.4 and 5,149 Bq m^{-2} , with a mean value of 216 Bq m^{-2} (CV: 208%), whereas in the soil samples the ^{137}Cs inventories ranged between 16 and 34,627 Bq m^{-2} , with a mean value of 1,602 Bq m^{-2} (CV: 237%). The differences in ^{137}Cs inventory between the different plots were statistically significant ($p < 0.05$) although different homogeneous groups were distinguished for the leaf and soil samples (Table 4; see box plots in Supplementary Fig. 4). Related to the leaf samples,

the control and the Th_2 plots had the highest values of ^{137}Cs inventory, while the remaining seven plots had much lower values, between -35% and -89% on average. Weighing the soil samples, six out of eight plots with decontamination practices presented higher values of ^{137}Cs inventory than the control plots; only the CC+LR_2 and CC+LR_3 plots had lower values of ^{137}Cs inventory. Over the test period and accounting the soil and leaf samples of the ten plots, the total (soil and leaf) ^{137}Cs inventories decreased by 49% in 2014 (mean $1,330 \text{ Bq m}^{-2} \text{ survey}^{-1}$) and 66% in 2015 (mean $878 \text{ Bq m}^{-2} \text{ survey}^{-1}$) related to the ^{137}Cs inventories in 2013 (mean $2,591 \text{ Bq m}^{-2} \text{ survey}^{-1}$). Mirroring the evolution of the radiocesium activities, the decrease of ^{137}Cs inventory was lower in 2015 than in 2014 and related to the previous year. During TSC_min the ^{137}Cs inventories in the leaf samples was 110% higher (mean $344 \text{ Bq m}^{-2} \text{ survey}^{-1}$) than during TSC_max (mean $164 \text{ Bq m}^{-2} \text{ survey}^{-1}$). Conversely, the ^{137}Cs movement in the soil samples was 43% lower during TSC_min (mean $1,306 \text{ Bq m}^{-2} \text{ survey}^{-1}$) than during TSC_max (mean $2,298 \text{ Bq m}^{-2} \text{ survey}^{-1}$).

The values and the temporal evolution of the daily movement of soil and leaf and of the ^{137}Cs inventories were presented in Fig. 5. The total daily discharge of soil and leaf over the test period and in the ten plots ranged between 0.04 and $155.1 \text{ g m}^{-2} \text{ day}^{-1}$ (mean $4.7 \text{ g m}^{-2} \text{ day}^{-1} \pm 297\% \text{ CV}$). The daily discharge of ^{137}Cs ranged between 0.2 and $4,961 \text{ Bq m}^{-2} \text{ day}^{-1}$ (mean $132 \text{ Bq m}^{-2} \text{ day}^{-1} \pm 299\% \text{ CV}$; see box plots in Supplementary Fig. 5). We observed a good potential correlation ($R^2: 0.9084$) among the total daily movement of leaf and soil and the total daily inventory of ^{137}Cs . The mean daily discharge of soil and leaf and of ^{137}Cs decreased over the test period, with maximum values in 2013 (mean $8.1 \text{ g m}^{-2} \text{ day}^{-1}$ and $235 \text{ Bq m}^{-2} \text{ day}^{-1}$); lower values in 2014 (-72% and -73%), and much lower values in 2015 (-53% and -68% related to 2014). During the three TSC_min periods the mean daily discharges of soil and leaf and of ^{137}Cs were 7% ($4.7 \text{ g m}^{-2} \text{ day}^{-1}$) and 28% ($106 \text{ Bq m}^{-2} \text{ day}^{-1}$) lower than during the three TSC_max periods ($5.0 \text{ g m}^{-2} \text{ day}^{-1}$ and $147 \text{ Bq m}^{-2} \text{ day}^{-1}$). The differences in the daily ^{137}Cs movement between the different plots were statistically significant ($p < 0.05$) and the same homogeneous groups were distinguished as those observed in the ^{137}Cs inventories for the leaf and soil samples. The highest discharge rates of ^{137}Cs appeared in the Th+LR_1 and Th+LR_2 plots (between 350 and $380 \text{ Bq m}^{-2} \text{ day}^{-1}$ on average), followed by the Th_1 and Th_2 plots (between 163 and $174 \text{ Bq m}^{-2} \text{ day}^{-1}$ on average). The CC+LR_1 ($104 \text{ Bq m}^{-2} \text{ day}^{-1}$ on average) and the LR ($92 \text{ Bq m}^{-2} \text{ day}^{-1}$ on average) plots also had higher rates than those obtained in the control plots ($51 \text{ Bq m}^{-2} \text{ day}^{-1}$ on average); whereas the CC+LR_2 ($19 \text{ Bq m}^{-2} \text{ day}^{-1}$ on average) and the CC+LR_3 ($25 \text{ Bq m}^{-2} \text{ day}^{-1}$ on average) plots were the only plots that had lower rates than the control plots.

3.3. Discussion

The increase of the daily overland flow discharge rates observed in the plots with decontamination practices and without presence of matting agreed with the results of [Dung et al. \(2011\)](#) in cypress plantations in two small catchments in south central Japan. These authors observed that overland flow increased between 4.8% and 7.4% after forest thinning. [Nanko et al. \(2016\)](#) also detected an increase in the throughfall fraction (from 58% to 79%) in a mature Japanese cypress forest in southern Japan after thinning. [Nam et al. \(2016\)](#) examined changes in suspended-sediment yields (SSY) after a 50% strip thinning in a Japanese cedar and cypress plantation forest in central Japan Tochigi revealing that SSY increased 17.0-fold compared with the pre-thinning period. Recently, [López-Vicente et al. \(2017\)](#) observed an increase of hydrological connectivity at hillslope and stream scales owing to tree thinning and new skidding trails in a forest plantation in central Japan, whereas progressive vegetation recovery one year after forest management operations triggered a reduction of hydrological connectivity in all compartments. The annual proportions of contribution of ^{137}Cs discharge by suspended sediment and leaf fraction were 96.7% and 3.3%, 96.5% and 3.5%, and 95.0% and 5.0% in 2013, 2014 and 2015, respectively. These results agreed with the proportions observed by [Iwagami et al. \(2017a\)](#) at stream sites in three headwater catchments located ~35 km northwest of the FDNPP, where ^{137}Cs discharge by suspended sediment, coarse organic matter, and dissolved fraction were 96–99%, 0.0092–0.069%, and 0.73–3.7%, respectively.

Tree thinning (Th plots) and litter removal (LR plot) resulted in mean increases of the total discharge rates of soil and leaf of 244% and 76%; and of ^{137}Cs inventories of 228% and 80% related to the control plots. The combined effect of both practices (Th+LR plots) triggered mean increases of the discharge rates of 532% of the total material and of 612% of the total ^{137}Cs inventories ([Table 4](#)). The three plots devoted to clearcutting (CC+LR) practices showed clear differences between them owing to the presence of matting. The CC+LR plot without matting had total discharge rates of soil and leaf, and of ^{137}Cs inventories 113% and 102% higher than the control plots. However, the two CC+LR plots with matting had mean decreases of the total discharge rates of soil and leaf of 52%; and of ^{137}Cs inventories of 58% related to the control plots. These results were in agreement with those observed by [Yang et al. \(2016\)](#) in rice paddies in Fukushima Prefecture, where surface-soil-removal caused the exponentially decreased of radiocesium (^{134}Cs and ^{137}Cs) activity in suspended sediment in irrigation water. [Iijima et al. \(2013\)](#) evaluated the effectiveness of decontaminating (by cutting down) a highly polluted evergreen forest located 1.3 km southwest of the FDNPP, concluding that radiocesium was mostly adsorbed on the surface of trees and partly penetrated into the trunks through the bark;

stripping contaminated topsoil and pruning the trees also reduced the air dose rates although in a minor way. [Teramage et al. \(2014b\)](#) studied the radiocesium concentration in the forest floor components (understory plants, litter and fermented layers) in a cypress plantation affected by the FDNPP accident in central Japan, observing that 99% of the total soil inventory of the Fukushima-derived and of the pre-Fukushima ^{137}Cs was in the upper 10 cm, suggesting the subsequent distribution most likely depends on the overland flow processes. In forest environments polluted by the Chernobyl accident, [Guillitte et al. \(1993\)](#) evaluated clearcutting as a highly effective short-term countermeasure to reduce the radionuclide air dose rates; although these authors highlighted the limitation of this technique that is only practicable for limited areas. More recently, [Ramzaev et al. \(2006\)](#) demonstrated the long-term stability and efficiency of the decontamination carried out in two Russian recreational areas located 180 km northeast of Chernobyl; where the levels of the ^{137}Cs content in grass, mushrooms and new generations of pines and birches from the treated plots were one or two orders of magnitude lower, than those registered in the samples from untreated areas. On the basis of these studies and our results we can conclude that the decontamination practices evaluated in this study were satisfactory and the new vegetation that will germinate in future will have much lower radiocesium rates. Additionally, the decrease trend in radiocesium concentration in the forest floor, owing to the vegetation recovery after the countermeasures, will reduce the possibility of the second pollution of the neighbouring residential and/or agricultural areas.

4. Conclusions

Despite the high temporal variability in the amount of soil and leaf collected in the ten experimental plots statistically significant differences in radiocesium activities were observed in the soil and leaf samples for ^{137}Cs and over the test period. The highest discharge rates of ^{137}Cs appeared in the two plots devoted to tree thinning and litter removal, highlighting the effectiveness of this decontamination practice to reduce the ambient dose rates. The two plots managed with tree thinning also presented high discharge rates. The plots managed with litter removal, and clearcutting with litter removal had higher radiocesium discharge rates than the rates measured in the two control plots. Matting induced lower discharge rates than in the control plots, appearing this technique as the most effective method to reduce a second influx of radiocesium from forest floor into neighbouring residential areas via overland flow. The observed temporal variability in both the total amount of soil and leaf, and radiocesium concentration was explained by (i) the different rainfall depths registered during the

measurement intervals; and (ii) the fluctuations of the total surface coverage between the periods with minimum and maximum vegetation coverage. The vegetation recovery after the countermeasures explained the decrease trend in radiocesium concentration that was very high in 2013, high in the first half of 2014, moderate in the second half of 2014, and low in 2015. This tendency will reduce the off-site consequences of radiocesium discharge from the forest floor. The contribution of ^{137}Cs discharge by soil was very high whereas the ^{137}Cs discharge by leaf fraction was small.

Acknowledgements

This research was funded by the project “Development of techniques for migration control against radioactive substances in forests (2012-2016)” of the Japanese Forestry Agency. Dr. Manuel López-Vicente acknowledges the financial support of his postdoctoral stay at the University of Tsukuba (Prof. Onda Laboratory) in 2015 to the Canon Foundation in Europe (Research Fellowships Program, Call 2014) and in 2016 to Prof. Yuichi Onda.

Appendix A. Supplementary content

Supplementary Figure 1: Location of the study area on the distribution map of deposition densities of radiocesium (^{134}Cs + ^{137}Cs) obtained from the 3rd airborne monitoring survey (MEXT; July 2, 2011; <http://ramap.jmc.or.jp/map/eng/>). Supplementary Figure 2: Location of the experimental plots in the stand A of the Kawauchi forest plantation (a). Pictures of the thinning_1 plot (logged area) taken at four dates: 2013.07.26, 2014.07.25, 2015.01.30 and 2015.06.25 (b). Supplementary Figures 3, 4 and 5: Box plots of radiocesium activities and inventory, and of the total weight and radiocesium discharge rates measured in the leaf and soil samples at the eight decontamination and the two control plots. Mean values in red colour.

References

- Achim, P., Monfort, M., Le Petit, G., Gross, P., Douysset, G., Taffary, T., Blanchard, X., Moulin, C., 2012. Analysis of radionuclide releases from the Fukushima Dai-ichi Nuclear Power Plant accident – Part II. Pure Appl. Geophys. 171 (3–5), 645–667. <http://dx.doi.org/10.1007/s00024-012-0578-1>.
- Aliyu, A.S., Evangeliou, N., Mousseau, T.A., Wu, J., Ramli, A.T., 2015. An overview of current knowledge concerning the health and environmental consequences of the Fukushima Daiichi Nuclear Power Plant (FDNPP) accident. Environ. Int. 85, 213–228.

- Cresswell, A.J., Kato, H., Onda, Y., Nanba, K., 2016. Evaluation of forest decontamination using radiometric measurements. *J. Environ. Radioactiv.* 164, 133–144.
- Dung, B.X., Miyata, S., Gomi, T., 2011. Effect of forest thinning on overland flow generation on hillslopes covered by Japanese cypress. *Ecohydrology* 4, 367–378.
- Guillitte, O., Tikhomirov, F.A., Shaw, G., Johanson, K., Dressier, A.J., Melin, J., 1993. Decontamination methods for reducing radiation doses arising from radioactive contamination of forest ecosystems- a summary of available countermeasures. *Sci. Total Environ.* 137(1–3), 307–314.
- Hashimoto, S., Ugawa, S., Nanko, K., Shichi, K., 2012. The total amounts of radioactively contaminated materials in forests in Fukushima, Japan. *Sci. Rep.* 2, 416.
- Iijima, K., Funaki, H., Tokizawa, T., Nakayama, S., 2013. Distribution of radioactive cesium in trees and effect of decontamination of forest contaminated by the Fukushima nuclear accident. *Proceedings of the International Conference on Radioactive Waste Management and Environmental Remediation, ICEM 2, V002T04A004.*
- Iwagami, S., Onda, Y., Tsujimura, M., Abe, Y., 2017a. Contribution of radioactive ^{137}Cs discharge by suspended sediment, coarse organic matter, and dissolved fraction from a headwater catchment in Fukushima after the Fukushima Dai-ichi Nuclear Power Plant accident. *J. Environ. Radioactiv.* 166(3), 466–474.
- Iwagami, S., Tsujimura, M., Onda, Y., Nishino, M., Konuma, R., Abe, Y., Hada, M., Pun, I., Sakaguchi, A., Kondo, H., Yamamoto, M., Miyata, Y., Igarashi, Y., 2017b. Temporal changes in dissolved ^{137}Cs concentrations in groundwater and stream water in Fukushima after the Fukushima Dai-ichi Nuclear Power Plant accident. *J. Environ. Radioactiv.* 166(3), 458–465.
- Iwagami, S., Onda, Y., Tsujimura, M., Hada M., Pun, I., 2017c. Vertical distribution and temporal dynamics of dissolved ^{137}Cs concentrations in soil water after the Fukushima Dai-ichi Nuclear Power Plant accident. *Environ. Pollut.* 230, 1090–1098.
- Kato, H., Onda, Y., Teramaga, M., 2012a. Depth distribution of ^{137}Cs , ^{134}Cs , and ^{131}I in soil profile after Fukushima Dai-ichi Nuclear Power Plant Accident. *J. Environ. Radioactiv.* 111, 59–64.
- Kato, H., Onda, Y., Gomi, T., 2012b. Interception of the Fukushima reactor accident-derived ^{137}Cs , ^{134}Cs and ^{131}I by coniferous forest canopies. *Geophys. Res. Lett.* 39, L20403.
- Kato, H., Onda, Y., Hisadome, K., Loffredo, N., Kawamori, A., 2017. Temporal changes in radiocesium deposition in various forest stands following the Fukushima Dai-ichi Nuclear Power Plant accident. *J. Environ. Radioactiv.* 166(3), 449–457.
- Kinouchi, T., Yoshimura, K., Omata, T., 2015. Modeling radiocesium transport from a river catchment based on a physically-based distributed hydrological and sediment erosion model. *J. Environ. Radioactiv.* 139, 407–415.
- Lepage, H., Laceby, J.P., Bonté, P., Joron, J.L., Onda, Y., Lefèvre, I., Ayrault, S., Evrard, O., 2016. Investigating the source of radiocesium contaminated sediment in two Fukushima coastal catchments with sediment tracing techniques. *Anthropocene* 13, 57–68.
- López-Vicente, M., Sun, X., Onda, Y., Kato, H., Gomi, T., Hiraoka, M., 2017. Effect of tree thinning and skidding trails on hydrological connectivity in two Japanese forest catchments. *Geomorphology* 292, 104–114.

- Mahara, Y., Ohta, T., Ogawa, H., Kumata, A., 2014. Atmospheric direct uptake and long-term fate of radiocesium in trees after the Fukushima nuclear accident. *Sci. Rep.* 4, 7121.
- Matsuda, N., Mikami, S., Shimoura, S., Takahashi, J., Nakano, M., Shimada, K., Uno, K., Hagiwara, S., Saito, K., 2015. Depth profiles of radioactive cesium in soil using a scraper plate over a wide area surrounding the Fukushima Dai-ichi Nuclear Power Plant, Japan. *J. Environ. Radioactiv.* 139, 427–434.
- Mikami, S., Maeyama, T., Hoshide, Y., Sakamoto, R., Sato, S., Okuda, N., Demongeot, S., Gurriaran, R., Uwamino, Y., Kato, H., Fujiwara, M., Sato, T., Takemiya, H., Saito, K., 2015. Spatial distributions of radionuclides deposited onto ground soil around the Fukushima Dai-ichi Nuclear Power Plant and their temporal change until December 2012. *J. Environ. Radioactiv.* 139, 320–343.
- Morino, Y., Ohara, T., Nishizawa, M., 2011. Atmospheric behavior, deposition, and budget of radioactive materials from the Fukushima Daiichi nuclear power plant in March 2011. *Geophys. Res. Lett.* 38(7), L00G11.
- Nam, S., Hiraoka, M., Gomi, T., Dung, B.X., Onda, Y., Kato, H., 2016. Suspended-sediment responses after strip thinning in headwater catchments. *Landsc. Ecol. Eng.* 12, 197–208.
- Nanko, K., Onda, Y., Kato, H., Gomi, T., 2016. Immediate change in throughfall spatial distribution and canopy water balance after heavy thinning in a dense mature Japanese cypress plantation. *Ecohydrology* 9(2), 300–314.
- Onda, Y., Gomi, T., Mizugaki, S., Nonoda, T., Sidle, R., 2010. An overview of the field and modelling studies on effects of forest devastation on flooding and environmental issues. *Hydrol. Process.* 24(5), 527–534.
- Orita, M., Nakashima, K., Taira, Y., Fukuda, T., Fukushima, Y., Kudo, T., Endo, Y., Yamashita, S., Takamura, N., 2017. Radiocesium concentrations in wild mushrooms after the accident at the Fukushima Daiichi Nuclear Power Station: Follow-up study in Kawauchi village. *Sci. Rep.* 7(1), Article number 6744.
- Ramzaev, V., Andersson, K.G., Barkovsky, A., Fogh, C.L., Mishine, A., Roed, J., 2006. Long-term stability of decontamination effect in recreational areas near the town Novozybkov, Bryansk Region, Russia. *J. Environ. Radioactiv.* 85(2-3), 280–298.
- Saegusa, J., Tagawa, A., Kurikami, H., Iijima, K., Yoshikawa, H., Tokizawa, T., Nakayama, S., Ishida, J., 2015. Radioactivity decontamination in and around school facilities in Fukushima (Conference Paper). *Proceedings of the 23rd International Conference on Nuclear Engineering: Nuclear Power - Reliable Global Energy, ICONE 2015; Makuhari Messe Chiba, Japan; Code 118695.*
- Saito, K., Tanihata, I., Fujiwara, M., Saito, T., Shimoura, S., Otsuka, T., Onda, Y., Hoshi, M., Ikeuchi, Y., Takahashi, F., Kinouchi, N., Saegusa, J., Seki, A., Takemiya, H., Shibata, T., 2014. Detailed deposition density maps constructed by large-scale soil sampling for gamma-ray emitting radioactive nuclides from the Fukushima Dai-ichi Nuclear Power Plant accident. *J. Environ. Radioactiv.* 139, 308–319.
- Sakai, M., Gomi, T., Nunokawa, M., Wakahara, T., Onda, Y., 2014. Short communication. Soil removal as a decontamination practice and radiocesium accumulation in tadpoles in rice paddies at Fukushima. *Environ. Pollut.* 187, 112–115.

- Takahashi, J., Tamura, K., Suda, T., Matsumura, R., Onda, Y., 2015. Vertical distribution and temporal changes of ^{137}Cs in soil profiles under various land uses after the Fukushima Dai-ichi Nuclear Power Plant accident. *J. Environ. Radioactiv.* 139, 351–361.
- Teramage, M.T., Onda, Y., Kato, H., Gomi, T., 2014a. The role of litterfall in transferring Fukushima-derived radiocesium to a coniferous forest floor. *Sci. Total Environ.* 490, 435–439.
- Teramage, M.T., Onda, Y., Patin, J., Kato, H., Gomi, T., Nam, S., 2014b. Vertical distribution of radiocesium in coniferous forest soil after the Fukushima nuclear power plant accident. *J. Environ. Radioactiv.* 137, 37–45.
- Yamashiki, Y., Onda, Y., Smith, H.G., Blake, W.H., Wakahara, T., Igarashi, Y., Matsuura, Y., Yoshimura, K., 2014. Initial flux of sediment-associated radiocesium to the ocean from the largest river impacted by Fukushima Daiichi Nuclear Power Plant. *Sci. Rep.* 4, 3714.
- Yang, B., Onda, Y., Wakiyama, Y., Yoshimura, K., Sekimoto, H., Ha, Y., 2016. Temporal changes of radiocesium in irrigated paddy fields and its accumulation in rice plants in Fukushima. *Environ. Pollut.* 208, 562–570.
- Yasutaka, T., Iwasaki, Y., Hashimoto, S., Naito, W., Ono, K., Kishimoto, A., Yoshida, K., Murakami, M., Kawaguchi, I., Oka, T., Nakanishi, J., 2013. A GIS-based evaluation of the effect of decontamination on effective doses due to long-term external exposures in Fukushima. *Chemosphere* 93 (6), 1222–1229.
- Yasutaka, T., Naito, W., 2016. Assessing cost and effectiveness of radiation decontamination in Fukushima Prefecture, Japan. *J. Environ. Radioactiv.* 151, 512–520.
-

Table 1

Dates of operations and installation of the runoff plots.

Plot				Related operations to install the plots	
Name	Slope	Installation (yy.mm.dd)	Type	Tasks	Dates (yy.mm.dd)
Co_1	35°	2013.04.08	Control	No operation	-
Co_2	20°	2013.04.08			
LR	37°	2013.04.08	Litter removal	Litter removal	2012.12.16 – 2013.01.10
Th_1	11°	2013.07.19	Thinning: logged area	Line thinning (cable yarding with swing yarder)	2013.06.06-24
Th_2	22°	2013.07.19	Thinning: under remnant trees		
CC+LR_1	19°	2013.07.19	Clearcutting + Litter removal: no matting	Logging road construction	2012.12.11-15
				Litter removal	2012.12.16 – 2013.01.10
CC+LR_2	20°	2013.04.08	Clearcutting + Litter removal: matting with seeds	Clearcutting (ground skidding)	2013.03.9-13
				Planted oak and cedar seedlings	2013.04.06 – 2013.07.09
CC+LR_3	20°	2013.04.08	Clearcutting + Litter removal: matting without seeds	Partial covering with erosion control matting	2013.04.04
Th+LR_1	17°	2013.07.19	Thinning + Litter removal: logged area	Litter removal	2013.01.31 – 02.06
Th+LR_2	8°	2013.07.19	Thinning + Litter removal: under remnant trees	Line thinning (cable yarding with swing yarder)	2013.06.6-24

Fig. 1. Rainfall during the field survey intervals (1st row), physical coverage on the ground (2nd row) and surface coverage by vegetation (3rd row) at the experimental plots between May 2013 and December 2014.

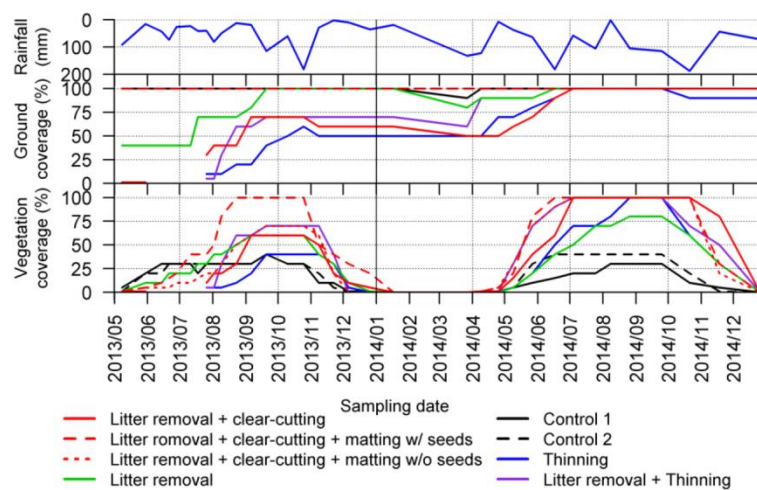


Fig. 2. Evolution in the dry weight (kg) and daily rainfall (mm day⁻¹) values (a), and ¹³⁷Cs activities (Bq kg⁻¹) (b) in the soil and leaf samples during the test period.

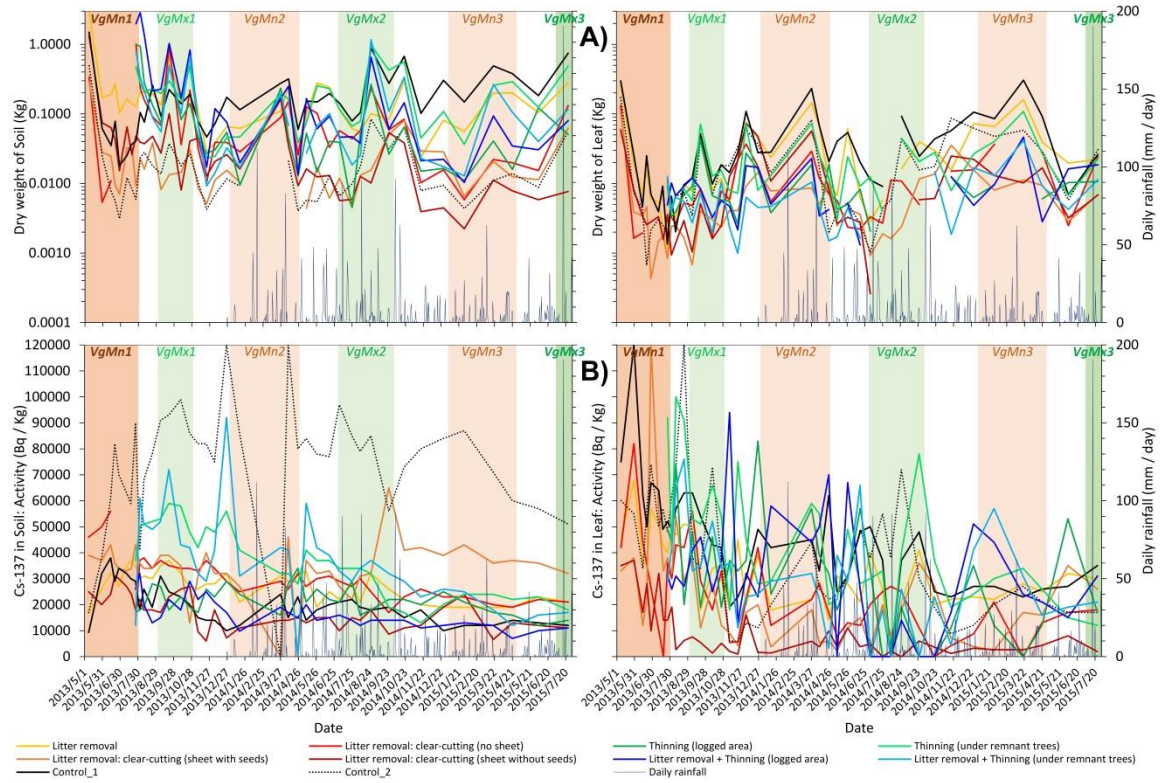


Fig. 3. Evolution in the relationship between the total surface cover (TSC: ground and vegetation coverage) and (i) the sediment yield (a); and (ii) the total (leaf and soil) radiocesium concentration (b) over the 39 field surveys.

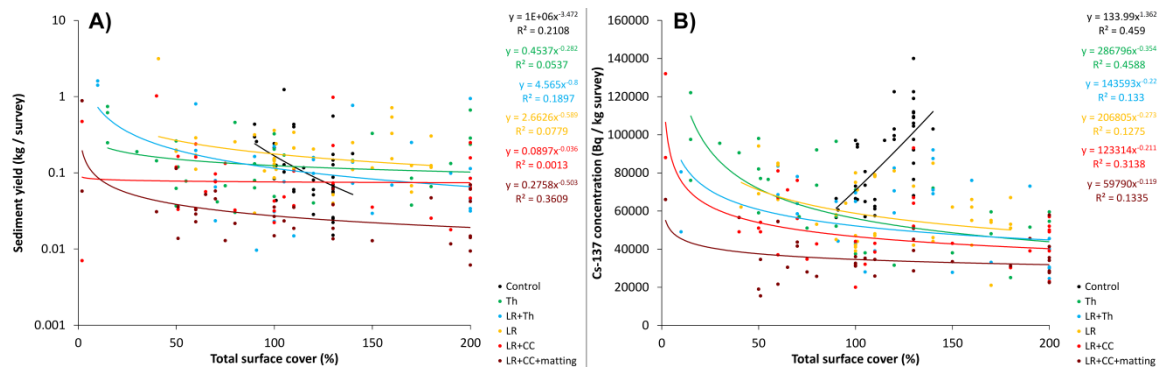


Table 2

Mean \pm CV (%) for radiocesium activities in the leaf and soil samples at the ten experimental plots and over the test period. Δ Co: change related to the average value at the control plots. Within column, values followed by the same letter are not significantly different between them at $p < 0.05$ (Holm-Sidak test).

Plot ID	¹³⁷ Cs activity (Bq / kg)			
	Leaf	Δ Co	Soil	Δ Co
Co_1	43,641 \pm 47%	-	19,982 \pm 38%	-
Co_2	38,377 \pm 63%	-	73,974 \pm 31%	-
<i>Control</i>	<i>41,009a \pm 55%</i>	-	<i>46,978a \pm 68%</i>	-
LR	32,667b \pm 42%	-20%	27,077c \pm 21%	-42%
CC+LR_1	23,763c \pm 72%	-42%	30,057c \pm 29%	-36%
CC+LR_2	22,741c \pm 93%	-45%	33,897b \pm 33%	-28%
CC+LR_3	8,582d \pm 113%	-79%	16,974d \pm 39%	-64%
Th_1	29,969b \pm 72%	-27%	21,500cd \pm 24%	-54%
Th_2	42,281a \pm 59%	3%	36,438b \pm 36%	-22%
Th+LR_1	29,938b \pm 76%	-27%	16,556d \pm 35%	-65%
Th+LR_2	29,272b \pm 66%	-29%	36,281b \pm 51%	-23%

Table 3

Mean and median (between brackets) for radiocesium activities in the leaf and soil samples during the periods of minimum and maximum total surface coverage (TSC) in the ten experimental plots.

Plot ID	¹³⁷ Cs activity (Bq / kg)			
	Leaf		Soil	
	TSCmin	TSCmax	TSCmin	TSCmax
Co_1	53,133 (50,000)	40,900 (42,500)	23,020 (24,000)	21,000 (20,500)
Co_2	41,000 (44,000)	43,100 (38,000)	65,600 (70,000)	82,200 (85,500)
<i>Control</i>	<i>47,067 (48,500)</i>	<i>42,000 (38,000)</i>	<i>44,310 (33,000)</i>	<i>51,600 (41,000)</i>
LR	35,533 (35,000)	29,500 (32,000)	27,267 (29,000)	28,100 (27,500)
CC+LR_1	28,818 (22,000)	26,200 (25,000)	30,818 (26,000)	28,900 (29,500)
CC+LR_2	28,020 (18,000)	20,010 (19,000)	32,533 (36,000)	33,500 (32,000)
CC+LR_3	14,493 (9,900)	3,430 (3,500)	19,773 (20,000)	16,960 (16,000)
Th_1	28,125 (28,000)	20,200 (19,000)	21,625 (19,000)	20,700 (20,000)
Th_2	43,125 (32,000)	41,700 (45,500)	30,000 (30,000)	38,900 (34,000)
Th+LR_1	42,750 (44,000)	19,400 (19,500)	14,850 (14,000)	16,500 (14,500)
Th+LR_2	27,400 (29,000)	21,900 (23,500)	22,625 (21,500)	39,100 (35,500)

Fig. 4. Evolution in the ^{137}Cs inventories (Bq m^{-2}) in the soil and leaf samples during the test period.

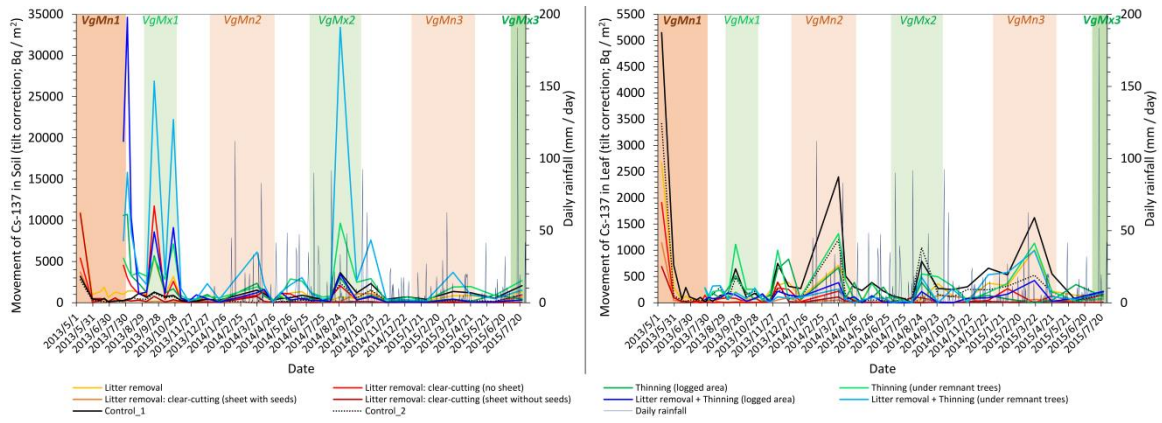
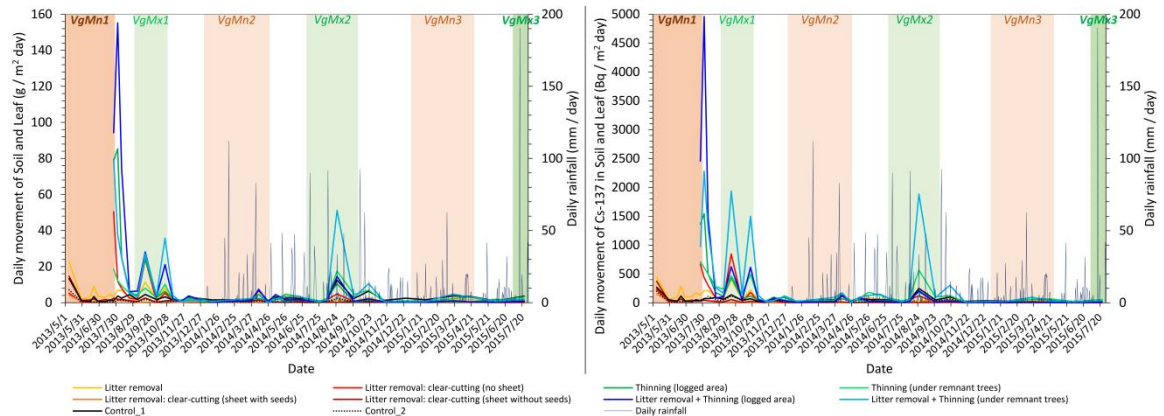


Table 4

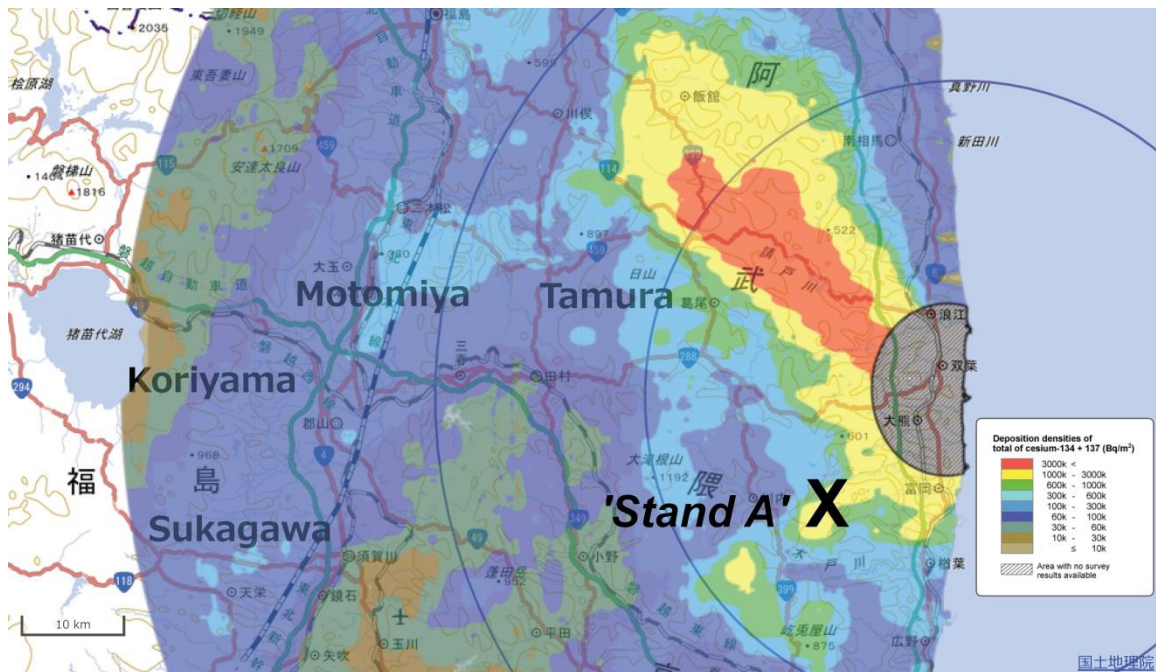
Mean \pm CV (%) for ^{137}Cs inventory and daily discharge rates in the soil and leaf samples at the ten experimental plots. ΔCo : change related to the average value at the control plots. Within column, values followed by the same letter are not significantly different between them at $p < 0.05$ (Holm-Sidak test).

Plot ID	^{137}Cs inventory				Daily discharge		
	Leaf	ΔCo	Soil	ΔCo	Total dry weight	^{137}Cs : Leaf	^{137}Cs : Soil
	(Bq / m^2)	%	(Bq / m^2)	%	($\text{g / m}^2 \text{ day}$)	($\text{Bq / m}^2 \text{ day}$)	($\text{Bq / m}^2 \text{ day}$)
Co_1	484 \pm 184%	-	838 \pm 95%	-	2.9 \pm 94%	20 \pm 136%	43 \pm 85%
Co_2	270 \pm 212%	-	487 \pm 121%	-	0.8 \pm 140%	12 \pm 165%	28 \pm 105%
Control	377a \pm 200%	-	663d \pm 108%	-	1.9d \pm 125%	16a \pm 151%	35d \pm 96%
LR	246b \pm 182%	-35%	1,280c \pm 145%	93%	3.3c \pm 124%	10b \pm 138%	82c \pm 116%
CC+LR_1	115c \pm 266%	-70%	1,185c \pm 180%	79%	4.0c \pm 231%	6c \pm 183%	98c \pm 190%
CC+LR_2	61d \pm 298%	-84%	322d \pm 189%	-51%	0.6d \pm 121%	3d \pm 222%	16d \pm 130%
CC+LR_3	43d \pm 291%	-89%	458d \pm 375%	-31%	1.2d \pm 188%	2d \pm 264%	23d \pm 250%
Th_1	194b \pm 111%	-48%	1,633c \pm 162%	146%	8.6b \pm 236%	11b \pm 116%	152b \pm 231%
Th_2	305ab \pm 116%	-19%	2,336b \pm 93%	252%	4.4c \pm 108%	16a \pm 119%	158b \pm 122%
Th+LR_1	108c \pm 97%	-71%	3,111ab \pm 228%	369%	13.7a \pm 243%	5c \pm 87%	345a \pm 283%
Th+LR_2	184b \pm 117%	-51%	5,106a \pm 160%	670%	10.0b \pm 180%	10b \pm 115%	370a \pm 173%

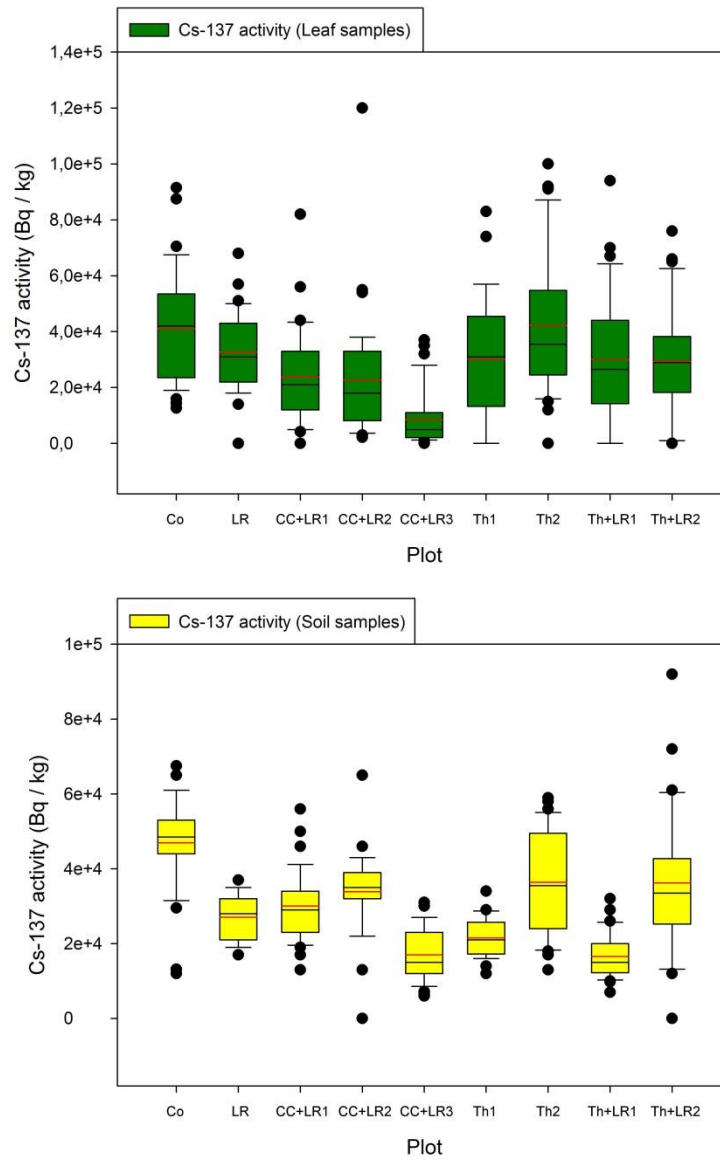
Fig. 5. Evolution in the daily discharge rates of soil and leaves ($\text{g m}^{-2} \text{day}^{-1}$) and total ^{137}Cs (in the soil and leaf samples; $\text{Bq m}^{-2} \text{day}^{-1}$) during the test period.



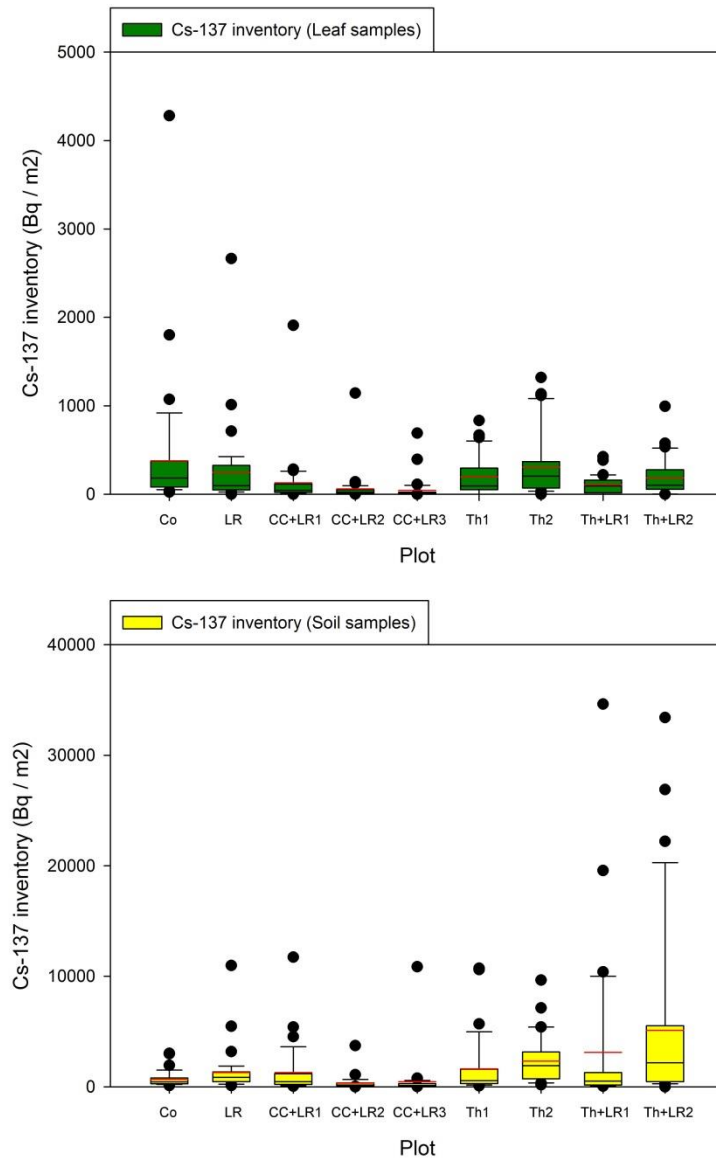
Supplementary Fig. 1. Location of the study area on the distribution map of deposition densities of radiocesium ($^{134}\text{Cs} + ^{137}\text{Cs}$) obtained from the 3rd airborne monitoring survey (MEXT; July 2, 2011; <http://ramap.imc.or.jp/map/eng/>).



Supplementary Fig. 3. Box plots of radiocesium activities measured in the leaf and soil samples at the eight decontamination and the two control (Co) plots. Mean values in red colour.



Supplementary Fig. 4. Box plots of radiocesium inventory measured in the leaf and soil samples at the eight decontamination and the two control (Co) plots. Mean values in red colour.



Supplementary Fig. 5. Box plots of the total weight and radiocesium discharge rates measured in the leaf and soil samples at the eight decontamination and the two control (Co) plots. Mean values in red colour.

